SUPPORTING MATERIALS AND METHODS

Mice

We compared mice whose β-cells 1) differed in the Cx36 gene dosage (Cx36+/+, Cx36+/-, Cx36 -/- ; 1-2); 2) were targeted, through the control of the Rat Insulin II Promoter (RIP; 3,4) for the β-cell-specific expression of transgenic Cx36 (RIP-Cx36+/-, RIP-Cx36+/+; 5). To this end, a 976 bp fragment of genomic rat Cx36, not including the intron of the Cx36 gene *Gjd2*, and corresponding to the full-length coding region (-3/+973; numbering from the translational start site) was subcloned into the expression vector pcDNA3.1 (Invitrogen). The transgene also contained intron and polyadenylation sequences from either human growth hormone (hGH; 4) or the rabbit β-globin gene (5, 6). Similar observations with regard to streptozotocin effects, cell-to-cell coupling and glycemia control, were made in all RIP-Cx36 mice, irrespective of the source of the intron and polyadenylation sequences, and thus all these animals are referred to as pertaining to the RIP-Cx36 line; 3) co-expressed Cx36 with either Cx32 (RIP-Cx32+/-, RIP-Cx32+/+; 4) or Cx43 (RIP-Cx43 +/-, RIP-Cx43+/+; 5), also targeted to β-cells through the use of RIP. The control mice of all lines, natively expressed Cx36. The native levels of this connexin were comparable in Cx36+/+ mice than in RIP-Cx36, -Cx32 and Cx43 -/- mice (Figure 1S). Cx36-/- mice did not express Cx36 (Fig 1S). Cx36 +/- featured levels of Cx36 which, within pancreatic islets, were intermediate between those of Cx36+/+ and Cx36-/- animals (Figure 1S). RIP-Cx36+/- and +/+ mice expressed higher levels of Cx36 than Cx36+/+ and RIP-Cx36-/- controls (Figure 1S). RIP-Cx32 and -Cx43 mice expressed Cx32 and Cx43 in addition to native Cx36, respectively (Figures 1S and 2S). The international nomenclature of the mouse lines, and the abbreviated names used in the text are given in Figure S3. Experiments were performed with null and transgenic mice that had been back crossed with C57BL/6J mice for 5-10 (Cx36) or 3-8 (RIP-Cx36, RIP-Cx2 and RIP-Cx43) generations. No significant difference was observed between the observations made in the former and latter mouse generations (not shown).

Islets and cells

Pancreatic islets were isolated by collagenase digestion and Histopaque enriched, as reported (4, 7). Islets were isolated, and cultured for 24 h in 1ml RPMI 1640 medium, supplemented with 10 %

FCS (8). Cells were dispersed from freshly isolated islets, as reported (8). Briefly, the islets were sequentially incubated in a Ca^{2+}-free medium for 5 min at room temperature, in the same medium supplemented with 3 mM EGTA for 15 min at room temperature, and in the latter medium containing 0.1 % trypsin (1 :250 ; Difco) for 6 min at 37°C. The cells were rinsed twice in sterile culture medium and plated at a density of 4 X 10^5 cells/ml on coverslips pre-coated with 804G matrix. After 8 hours, cells were exposed for 36 h to 1 ml either fresh medium or the mix of cytokines described in the text. The MIN6 (9) and INS-1E lines of insulin-producing cells (10), which natively express Cx36 (11, 12), were cultured for 3 days, as reported (11, 12).

Cell cloning, transfection and analysis

To identify Cx36 over expressing clones of MIN6 cells, the wild type population was diluted so as to plate 1 cell per well of 96 well plates. After 3 week culture, wells containing a single cluster were trypsinised, and the cells passed for expansion. Each cell population was then assessed for Cx36 expression by immunolabeling of cells and protein extracts, as described below. Clones that featured a Cx36 expression significantly higher than WT companion cells were repeatedly assessed every 3 months of culture. Clones that retained a stable expression of Cx36 over more than 2 years were selected for the experiments.

To generate stable MIN6 clones featuring a down-regulation of Cx36 expression, the full coding sequence of mouse Cx36 was inserted in an antisense orientation, using 2 EcoRI sites, within plasmid pcDNA3 (Invitrogen) which contains a CMV early promoter region and a neomycin-resistance gene. Subconfluent cultures of MIN6 cells were transfected with Polyfect Transfection reagent (Qiagen) as per the manufacturer's instructions. Stable transfectants were selected in the presence of 350 µg/mL Geneticin (G-418 sulfate; Gibco BRL). After 2 weeks of selection, single cells were plated, one cell per well, in 96-well plates, to allow for cloning of stable transfectants, as reported in the previous paragraph. For evaluating Cx36 distribution, over expressing, WT and antisense cells were plated at an initial density of 200 x 10^3 cells/ ml on glass coverslips pretreated with 804G matrix, cultured 3 days, and then exposed for 15h to either fresh culture medium or this medium supplemented with the 3 cytokines mentioned in the text. At this time, the medium of some of the cells was replaced with the Annexin V- EGFP / PI Apoptosis Detection Kit (BioVision)

solution, and processed as per the manufacturer's instructions. Control and cytokine-exposed cells were then fixed in 2% PFA for 15 min, rinsed, mounted on a microscope slide with a DAPI-containing antifading solution (ProTaqs® MountFluor Anti Fading, Quartett Immunodiagnostika) and photographed. Twenty fields were photographed on 2 coverslips per condition at the original magnification of 40x, and per condition to determine the percentage of apoptotic and necrotic cells. Quantitative analysis of the immunofluorescence images was carried out using the Metamorph/metaXpress software (Molecular Devices), to evaluate the volume density (Vv) of Cx36 per MIN6 cell cluster (given by the ratio of the areas positively stained by the anti Cx36 antibodies to the area of the cluster on which they projected). 40-160 clusters were evaluated per condition, in 4 independent experiments

To evaluate the effects of siRNAs targeting rat Cx36, INS1-E cells were transfected with 30 nM siRNA, using lipofectamin RNAi Max (Invitrogen), as previously described (13). Two siRNAs targeting Cx36 (Cx36 siRNA#1: 5'-GGUCCAGCUUCGAAGACAtt-3'; Cx36 siRNA#2: 5'-CCAUCUCCCAUAUACGUUAtt-3') were r*Gjd2 Silencer*® Select pre-designed (Ambion, Applied Biosystems). As control, we used an Allstars Negative Control siRNA (Qiagen), which has no effect on β-cell gene expression and viability (13, 14). After a 48h culture, the cells were collected and stained with the DNA-binding dyes Propidium Iodide (5 µg/ml) and Hoechst 33342 (5 µg/ml, Sigma-Aldrich), as previously reported (15). The cells were examined by inverted fluorescence microscopy (Axiovert 200, Carl Zeiss), and a minimum of 500 cells was scored per experiment by two independent observers, one of them unaware of sample identity, to determine the percentage of apoptotic (Hoechst 33342-stained) and necrotic cells (propidium iodide-stained). The necrosis levels were low (1.22±0.09 %), and similar under all conditions.

Histology

At sacrifice, pancreas were sampled, fixed in Bouin solution, embedded in paraffin and processed for standard histology and morphometric evaluation of β-cell mass in 5 µm thick sections (4, 7).

Immunofluorescence

Sections of pancreas or isolated islets from the various mouse genotypes were stained for 1) insulin, to evaluate the mass of β-cells; 2) GLUT2, since this glucose transporter also allows the uptake of STZ and AX by β-cells (16-18); 3) Cx36, Cx32, and Cx43, the 3 major connexins expressed in the pancreas (19), to evaluate the pattern of islet cell connexins; 4) cytochrome C, since this mitochondrial enzyme is known to reflect the activation of pro-apoptotic mechanisms involving a permeability transition of mitochondrial membranes (20, 21). Paraffin sections of pancreas and isolated islets, fixed in either Bouin's solution (for insulin and GLUT2 labeling) or 4% paraformaldehyde followed by a microwave antigen retrieval treatment (for cytochrome C labeling), as well as cryostat sections of unfixed tissue, were permeabilized in -20°C acetone (for Cx labeling), and immunostained as previously described (4,7). The following antibodies were used: guinea pig polyclonal 16D against insulin (4) diluted 1:700, rabbit polyclonal against mouse GLUT2 diluted 1:200 (17), rabbit polyclonal against Cx32 (Zymed, 71-0600) diluted 1:200, rabbit polyclonal against Cx43 (Zymed, 71-0700) diluted 1:100, rabbit polyclonal against Cx36 (Zymed, 51-6200) diluted 1:40, mouse monoclonal against cytochrome C (BD, 556433) diluted 1: 300. All incubations were performed for 2 h at room temperature, except for cytochrome C for which antibodies were applied for 15 h at 4°C. The sections were washed, exposed for 1 h to either a fluoresceinated or a rhodaminated antibody against guinea pig, mouse or rabbit IgGs, whichever appropriate, counterstained with 0.03% Evans' blue (4, 7), and photographed with an Axiophot fluorescence microscope (Zeiss).

Living and dead cell detection

In experiments testing the effects of STZ and AX, which kill β-cells by both apoptosis and necrosis (16-18), living and dead cells were differentiated within intact isolated islets using a calcein-ethidium bromide Live/Dead kit (Molecular Probes), and a LSM 510 confocal microscope (Zeiss). In this method, the AM form of calcein is de-esterified only by living cells, staining these in green fluorescence, whereas ethidium bromide permeates only dead cells, staining these in red fluorescence. In experiments testing the effects of pro-apoptotic cytokines (20-23), apoptosis was determined by TUNEL reaction (In Situ Cell Death Detection, Roche Diagnostics GmbH, Cat. No 1

684 795) on islet sections, as per the manufacturers' instructions. In this approach, apoptotic cells are stained in green by fluorescein. In experiments testing the effects of cytokines on primary cells dissociated from isolated islets, apoptosis and necrosis were differentiated using the Annexin V-EGFP Apoptosis Detection Kit (BioVision, Cat. No K104-400), as per the manufacturer's instructions. In this approach, which is most sensitive to detect the early apoptosis within pancreatic islets (23), Annexin V binds to the phosphatidylserine that is translocated from the cytoplasmic to the external leaflet of the cell membrane during early apoptosis, staining apoptotic cells by a green fluorescence. Propidium iodide permeates the ruptured membrane of necrotic cells, staining their nuclei by a red fluorescence. As shown in Figure S7, late apoptotic and necrotic cells are simultaneously labeled by the two tracers.

The tridimensional organization of isolated islets, does not allow for an easy counting of individual cells in sections. Thus, when intact islets were used, we scored the volumetric density (internationally referred to as volume density, and represented by the Vv symbol; 24, 25) of dead (in experiments testing STZ) or apoptotic cells (in experiments testing cytokines), i.e. the fraction of islet area occupied by calcein (STZ experiments) or TUNEL positive cells (cytokine experiments), as evaluated on sections by standard morphometric analysis (4, 24, 25). Data are reported as the dimensionless Vv value (24-26), which ranges from 0 to 1. In experiments dealing with single islet cells, the cells were fixed for 15 min in 2% paraformaldehyde in 0.1 M phosphate buffer at the end of the Annexin V-propidium iodide staining, detected under phase-contrast illumination, and scored for fluorescein and/or rhodamine signal. 3'000 single β-cells, identified under phase-contrast illumination, were scored per experiment to determine the proportion of Annexin V-EGFP (green membrane = early apoptosis) and propidium iodide-positive cells (red cytoplasms/nuclei = late apoptosis and necrosis).

Tracer microinjection

Isolated islets were attached to Sylgard- and poly-L-lysine-coated dishes, transferred on the heated stage (37^{o}C) of a Universal Zeiss microscope and kept in a Krebs Ringer bicarbonate HEPES buffer, pH 7.4, containing 117 mM NaCl, 4.7 mM KCl, 2.5 mM $CaCl_2$, 1.2 mM $MgSO_4$, 1.2 mM KH_2PO_4, 5.0 mM $NaHCO_3$, 10 mM HEPES, 10 mM glucose and 0.5% (wt/vol) BSA (2, 4, 7).

Individual cells located in the islet center were impaled using glass microelectrodes filled with a 4% solution of either Lucifer Yellow (LY; MW 443 for the anion with 2 negative charges) or Ethidium Bromide (EB; MW 314 for the cation with 1 positive charge), both in 150 mM LiCl (pH 7.2). After cell penetration, the tracers were iontophoretically injected for 5 min by applying 0.1 nA square pulses of 900 msec duration and 0.5-Hz frequency (2, 4, 7). Pulses were negative for injection of LY and positive for EB. In all cases, the extent of diffusion was captured with an Axiocam camera (Carl Zeiss SMT) coupled to the fluorescence microscope. The tridimensional organization of isolated islets, does not allow for an easy counting of individual labeled cells. Therefore, the extent of coupling was determined by measuring the area labeled by each tracer ("tracer labelled area" expressed in μm^2 in Figure 6), irrespective of whether there was cell-to-cell coupling or whether the injected cell was uncoupled (2, 4, 7). Measurements were made on digitized photographs of the intact islets, using a digitalizing tablet and the LeicaQWin software (Leica, Wetzlar). Immediately after the end of each experiment, we also scored whether a microinjection resulted The in the cell-to-cell transfer of either one of the 2 tracers tested (coupling), or whether the tracers were retained within the microinjected cell (uncoupling) (2, 4, 7).

Biochemistry

For evaluation of Cx36 levels, total RNA and proteins were analyzed by quantitative PCR and western blots, as reported (11, 12, 27, 28). Levels of Cx36 mRNA were evaluated relative to those of the ribosomal L27 mRNA, whereas those of Cx36 protein were evaluated relative to those of either tubulin (INS1-E cells) or actin (MIN6 cells), which were used as internal standards. All data are shown relative to the levels observed under control conditions, which were set to 1. To evaluate the total insulin content of pancreas, the whole glands were carefully dissected and extracted in acid-ethanol for 24h, as reported (2, 4, 7, 8). Insulin was measured by radioimmunoassay, using rat insulin as standard (2, 4, 7, 8).

Glucose influx

The incorporation of glucose by β-cells was determined by exposing isolated islets for 30 min at 37°C to 0.7 mM 6-(N-(7-nitrobenz-2-oxa-1,3-diazol-4-yl)amino)-6-deoxyglucose (NDBG; Molecular

Probes) (29, 30). Cells showing a detectable fluorescence signal were scored in 7-19 islets per group, and the percentage of stained cells reported in the legend to Figure S5.

Nitrite measurement

The production of NO in the presence and absence of cytokines was evaluated by the release of nitrite in the medium, which was measured after reaction with Griess reagent (31). Data were not normalized, and are shown as mean + SEM of the nitrite concentration in the medium bathing the isolated islets, and expressed in µM (Figure 4A and B).

REFERENCES

1. Güldenagel M, Ammermüller J, Feigenspan A, Teubner B, Degen J, Söhl G, Willecke K and Weiler R. Visual transmission deficits in mice with targeted disruption of the gap junction gene connexin36. *J Neurosci*. 2001;21:6036-6044.
2. Ravier MA, Güldenagel M, Charollais A, Gjinovci A, Caille D, Söhl G, Wollheim CB, Willecke K, Henquin JC, and Meda P. Loss of connexin36 channels alters beta-cell coupling, islet synchronization of glucose-induced Ca2+ and insulin oscillations, and basal insulin release. *Diabetes.* 2005;54:1798-1807.
3. Hanahan D. Heritable formation of pancreatic beta-cell tumours in transgenic mice expressing recombinant insulin/simian virus 40 oncogenes. *Nature.* 1985;315:115-122.
4. Charollais A, Gjinovci A, Huarte J, Bauquis J, Nadal A, Martin F, Andreu E, Sanchez-Andres JV, Calabrese A, Bosco D, Soria B, Wollheim CB, Herrera PL, and Meda P. Junctional communication of pancreatic beta cells contributes to the control of insulin secretion and glucose tolerance. *J Clin Invest.* 2000;106:235-243.
5. Klee P, Lamprianou S, Charollais A, Caille D, Sarro R, Cederroth M, Haefliger JA, Meda P. Connexin implication in the control of the murine beta-cell mass. Pediatr Res. 2011;70:142-147.
6. Beyer WR, Westphal M, Ostertag W, and Von Laer, D. Oncoretrovirus and lentivirus vectors pseudotyped with lymphocytic choriomeningitis virus glycoprotein: generation, concentration, and broad host range. *J Virol.* 2002;76:1488-1495.
7. Charpantier E, Cancela J and Meda P. Beta cells preferentially exchange cationic molecules via connexin 36 gap junction channels. *Diabetologia*.2007;50:2332-2341.
8. Meda P, Bosco D, Chanson M, Giordano E, Vallar L, Wollheim C, and Orci L. Rapid and reversible secretion changes during uncoupling of rat insulin-producing cells. *J Clin Invest.* 1990;86:759-768.
9. Miyazaki J, Araki K, Yamato E, Ikegami H, Asano T, Shibasaki Y, Oka Y, and Yamamura K. Establishment of a pancreatic beta cell line that retains glucose-inducible insulin secretion: special reference to expression of glucose transporter isoforms. *Endocrinology*.1990;127:126 -132.

10. Janjic D, Maechler P, Sekine N, Bartley C, Annen AS, and Wolheim CB. Free radical modulation of insulin release in INS-1 cells exposed to alloxan. *Biochem. Pharmacol.* 1999;57:639–648.

11. Calabrese A, Zhang M, Serre-Beinier V, Caton D, Mas C, Satin LS, and Meda P. Connexin 36 controls synchronization of Ca2+ oscillations and insulin secretion in MIN6 cells. *Diabetes*. 2003;52:417-424.

12. Le Gurun S, Martin D, Formenton A, Maechler P, Caille D, Waeber G, Meda P, and Haefliger JA. Connexin-36 contributes to control function of insulin-producing cells. *J Biol Chem.* 2003;278:37690-37697.

13. Moore F, Colli ML, Cnop M, Esteve MI, Cardozo AK, Cunha DA, Bugliani M, Marchetti P, and Eizirik DL. PTPN2, a candidate gene for type 1 diabetes, modulates interferon-gamma-induced pancreatic beta-cell apoptosis. *Diabetes.* 2009;58:1283-1291.

14. Moore F, Naamane N, Colli ML, Bouckenooghe T, Ortis F, Gurzov EN, Igoillo-Esteve M, Mathieu C, Bontempi G, Thykjaer T, Ørntoft TF, and Eizirik DL. STAT1 Is a Master Regulator of Pancreatic {beta}-Cell Apoptosis and Islet Inflammation. *J Biol Chem*. 2011;286:929-941.

15. Cardozo AK, Ortis F, Storling J, Feng YM, Rasschaert J, Tonnesen M, Van Eylen F, Mandrup-Poulsen T, Herchuelz A, and Eizirik DL. Cytokines downregulate the sarcoendoplasmic reticulum pump Ca2+ ATPase 2b and deplete endoplasmic reticulum Ca2+, leading to induction of endoplasmic reticulum stress in pancreatic beta-cells. *Diabetes*. 2005;54:452-461.

16. Lenzen S. The mechanisms of alloxan- and streptozotocin-induced diabetes. *Diabetologia*. 2008;51:216-226.

17. Elsner M, Guldbakke B, Tiedge M, Munday R, and Lenzen S. Relative importance of transport and alkylation for pancreatic beta-cell toxicity of streptozotocin. *Diabetologia*. 2002;43:1528-1533.

18. Hosokawa M, Dolci W, and Thorens B. Differential sensitivity of GLUT1- and GLUT2-expressing beta cells to streptozotocin. *Biochem Biophys Res Commun*. 2001;289:1114-1117.

19. Meda P, Pepper MS, Traub O, Willecke K, Gros D, Beyer E, Nicholson B, Paul D, and Orci L. Differential expression of gap junction connexins in endocrine and exocrine glands. *Endocrinology*. 1993;133:2371-2378.

20. Desagher S, and Martinou JC. Mitochondria as the central control point of apoptosis. *Trends Cell Biol*. 2000;10:369-377.

21. Bernardi P, and Rasola A. Calcium and cell death: the mitochondrial connection. *Subcell Biochem*. 2007;45:481-506.

22. Eizirik DL, and Mandrup-Poulsen T. A choice of death: the signal-transduction of immune-mediated beta-cell apoptosis. *Diabetologia*. 2001;44:2115-2133.

23. Cattan P, Berney T, Schena S, Molano RD, Pileggi A, Vizzardelli C, Ricordi C, Inverardi L. Early assessment of apoptosis in isolated islets of Langerhans. *Transplantation*. 2001;71:857-862.

24. Weibel ER. *Stereological methods*. London, England: Academic Press; 1979;1**:**26-30.

25. Underwood EE. A standardized system of notation for stereologists. *Stereologia*. 1964;3:5-7.

26. Stefan Y, Meda P, Neufeld M, and Orci L. Stimulation of insulin secretion reveals heterogeneity of pancreatic B cells in vivo. *J Clin Invest.* 1987;80:175-183.

27. Serre-Beinier V, Le Gurun S, Belluardo N, Trovato-Salinaro A, Charollais A, Haefliger JA, Condorelli DF, and Meda P. Cx36 preferentially connects beta-cells within pancreatic islets. *Diabetes.* 2000;49:727-734.

28. Serre-Beinier V, Bosco D, Zulianello L, Charollais A, Caille D, Charpantier E, Gauthier BR, Diaferia GR, Giepmans BN, Lupi R, Marchetti P, Deng S, Buhler L, Berney T, Cirulli V, and Meda P. Cx36 makes channels coupling human pancreatic beta-cells, and correlates with insulin expression. *Hum Mol Genet.* 2009;18:428-439.

29. Loaiza A, Porras OH, and Barros LF. Glutamate triggers rapid glucose transport stimulation in astrocytes as evidenced by real-time confocal microscopy. *J Neurosci.* 2003;23:7337-7342.

30. Rauchman MI, Wasserman JC, Cohen DM, Perkins DL, Hebert SC, Milford E, and Gullans SR. Expression of GLUT-2 cDNA in human B lymphocytes: analysis of glucose transport using flow cytometry. *Biochim Biophys Acta*. 1992;1111:231-238.

31. Green LC, Wagner D, Glogowski J, Skipper P, Wishnok J, and Tannenbaum S. Analysis of nitrate, nitrite, and [15N]nitrate in biological fluids. *Anal Biochem.* 1982;126:131-138.

SUPPORTING FIGURES AND LEGENDS

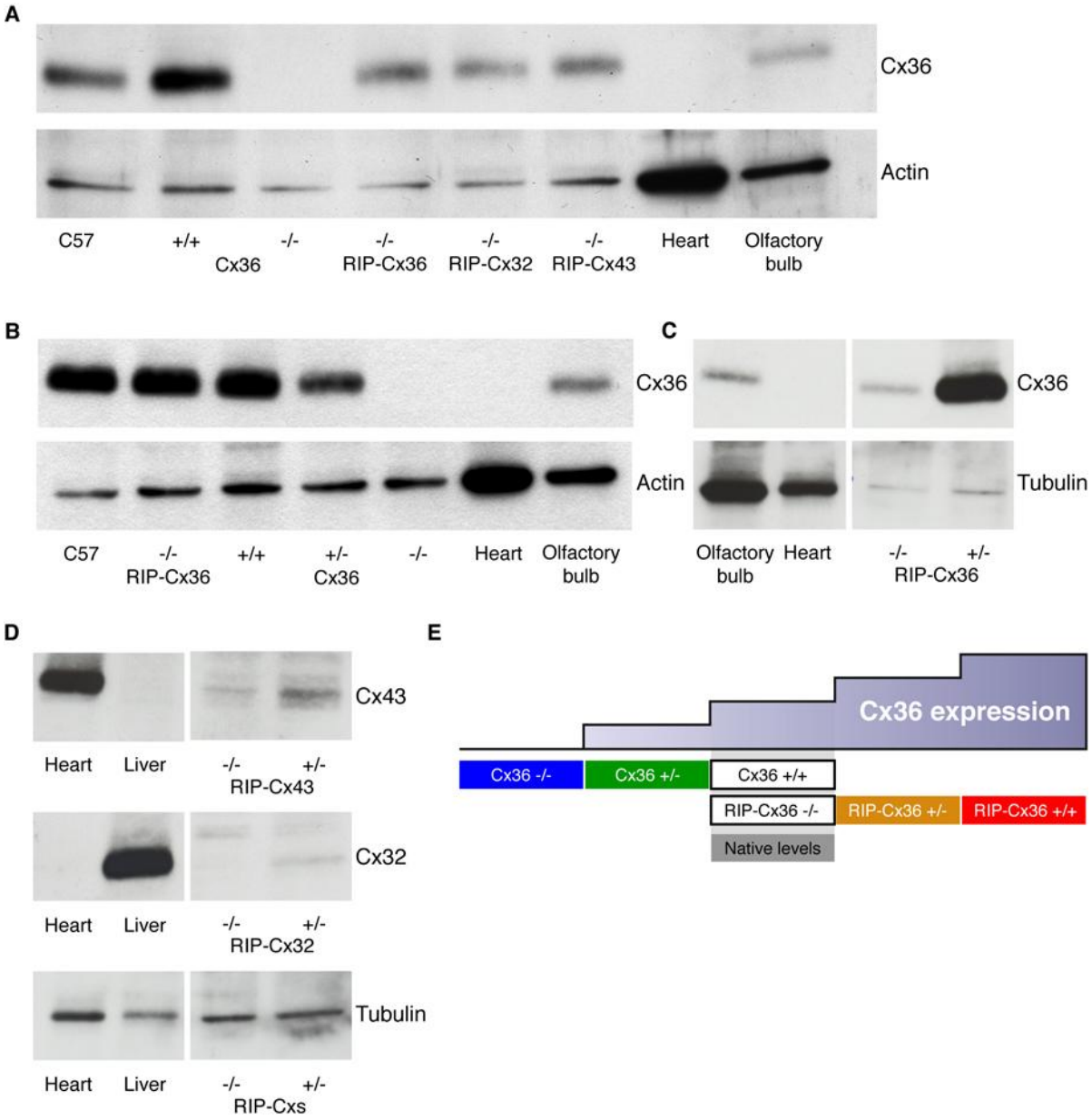

Figure S1: The pattern of islet cell connexins differs in the mouse lines we compared.
A) Immunoblotting of total islet extracts reveals the native presence of Cx36 in C57BL/6 mice (C57) and in all controls (Cx36+/+, RIP-Cx36-/-, RIP-Cx32 -/- and RIP-Cx43 -/-) of the mouse lines we compared. Cx36-/- mice did not express Cx36. **B)** The levels of Cx36 in islets of Cx36+/- mice were intermediate between those observed in Cx36+/+ and Cx36-/- littermates. **C)** RIP-Cx36+/- mice featured higher levels of Cx36 than -/- littermates **D)** Immunoblotting revealed traces of Cx43 (top panel) in total islet extracts of RIP-Cx43-/- mice, and higher levels of the connexin in RIP-Cx43+/- littermates. Immunoblotting revealed Cx32 (middle panel) in RIP-Cx32 +/-, but not RIP-Cx32-/- mice. Loading (10 µg/lane) was monitored with either α-actin (A, B) or tubulin (C and D). Extracts of heart, olfactory bulb and liver served as controls. E) Schematic view of the changes of Cx36 levels in the different mouse genotypes that we compared. **C-D)** Lanes were run on a same gel but were not contiguous.

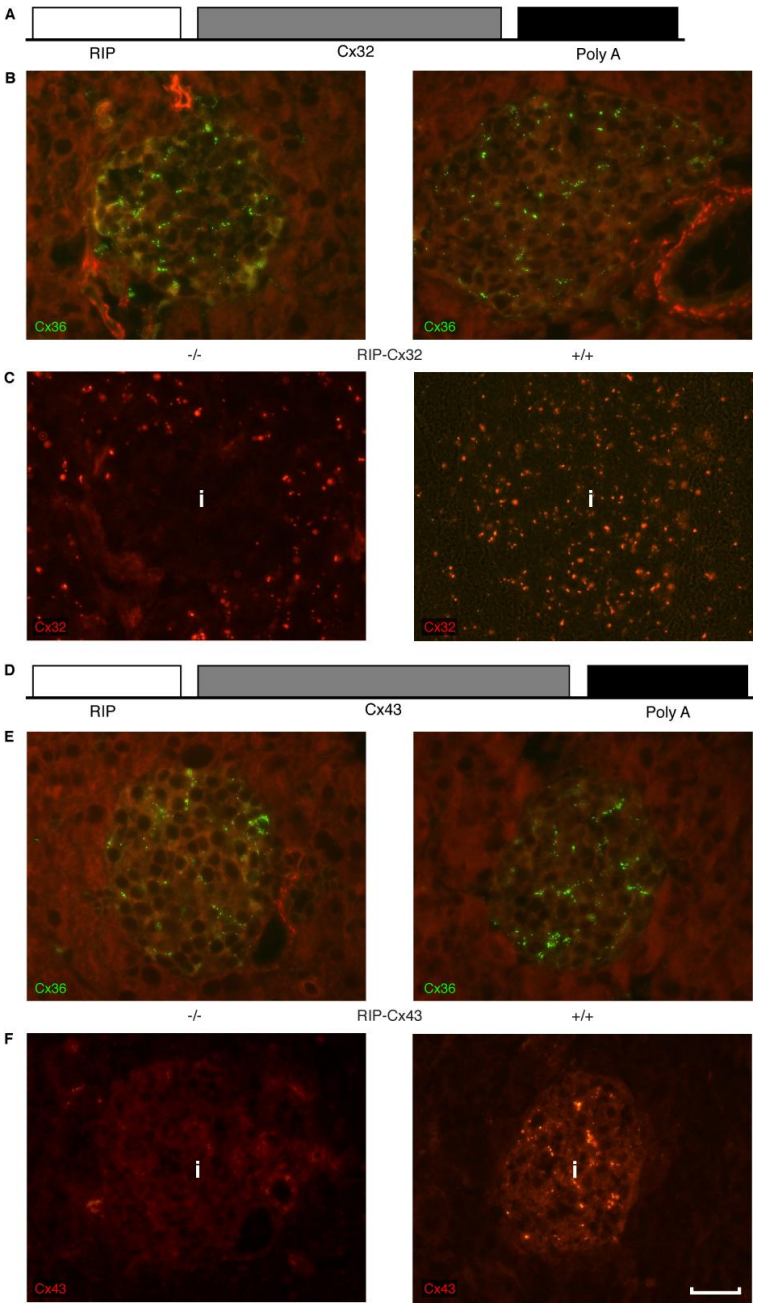

Figure S2: The β-cells of RIP-Cx32 and -Cx43 mice co-express Cx36 and either Cx32 or Cx43.

A) To generate RIP-Cx32 mice, we used the Rat Insulin II Promoter (RIP), a cDNA comprising the entire coding sequence of rat Cx32 (Cx32), and introns and polyA sequences from human growth hormone (Poly A). **B)** Immunofluorescence revealed a similar punctate distribution of Cx36 (green) within an islet of a control RIP-Cx32-/- (left panel) and a RIP-Cx32+/+ mouse (right panel). **C)** Immunostaining showed the abundant distribution of Cx32 (red) in the exocrine pancreas (left panel), and its absence in an endocrine islet (i) of a RIP-Cx32-/- mouse. In a RIP-Cx32+/+ mouse (right panel), Cx32 was abundant in both acini and islet (i). **D)** The construct used to generate RIP-Cx43 mice comprised the Rat Insulin II Promoter (RIP), a cDNA coding rat Cx43 (Cx43), and regulatory sequences of human growth hormone (Poly A). **E)** Immunofluorescence revealed the expression of Cx36 within an islet of a control RIP-Cx43-/- (left panel) and a +/+ mouse (right panel). **F)** Immunostaining did not detect Cx43 in either the exocrine acini or an endocrine islet (i) of a RIP-Cx43-/- mouse (left panel). In a RIP-Cx43+/+ mouse (right panel), Cx43 was still undetected in the exocrine pancreas, and became obvious in the central β-cells of an endocrine islet (i). The red background staining of all sections is due to the Evans' blue counterstain, which was used to decrease autofluorescence. Bar, 50 μm.

International nomenclature *	Abbreviated nomenclature used in paper	Genotype	Beta-cell Cx		
			Cx36	Cx32	Cx43
C57BL/6J	C57	+/+	++	-	-
C57BL/6J - TgH(Gjd2 ^{tm}) $^{1\ Kwi}$	Cx36	+/+	+++	-	-
		+/-	+	-	-
		-/-	-	-	-
C57BL/6J - TgN(RIP-Gjd2) ^{1Ugfm}	RIP-Cx36	-/-	++	-	-
		+/-	+++	-	-
		+/+	++++	-	-
C57BL/6J - TgN(RIP-Gja1) ^{1Ugfm}	RIP-Cx43	-/-	++	-	-
		+/-	++	-	+
		+/+	++	-	++
C57BL/6J - TgN(RIP-Gjb1) $^{1\ Ugfm}$	RIP-Cx32	-/-	++	-	-
		+/-	++	+	-
		+/+	++	++	-

* as per ILAR News, 34:3-10(1992). National Academy Press, Washington, D.C.

Figure S3: Nomenclature and main characteristics of the mouse lines we used

The table gives the international nomenclature of the mouse lines we studied, and the abbreviated nomenclature we used throughout the text. It further summarizes for each mouse genotype, the Cx pattern of β-cells, as deduced from immunolabeling of islet protein extracts and sections. Blue symbols reflect native β-cell levels. Red symbols outline the *de novo* expression of either Cx32 or Cx43. – not detectable; + to ++++ increasing levels.

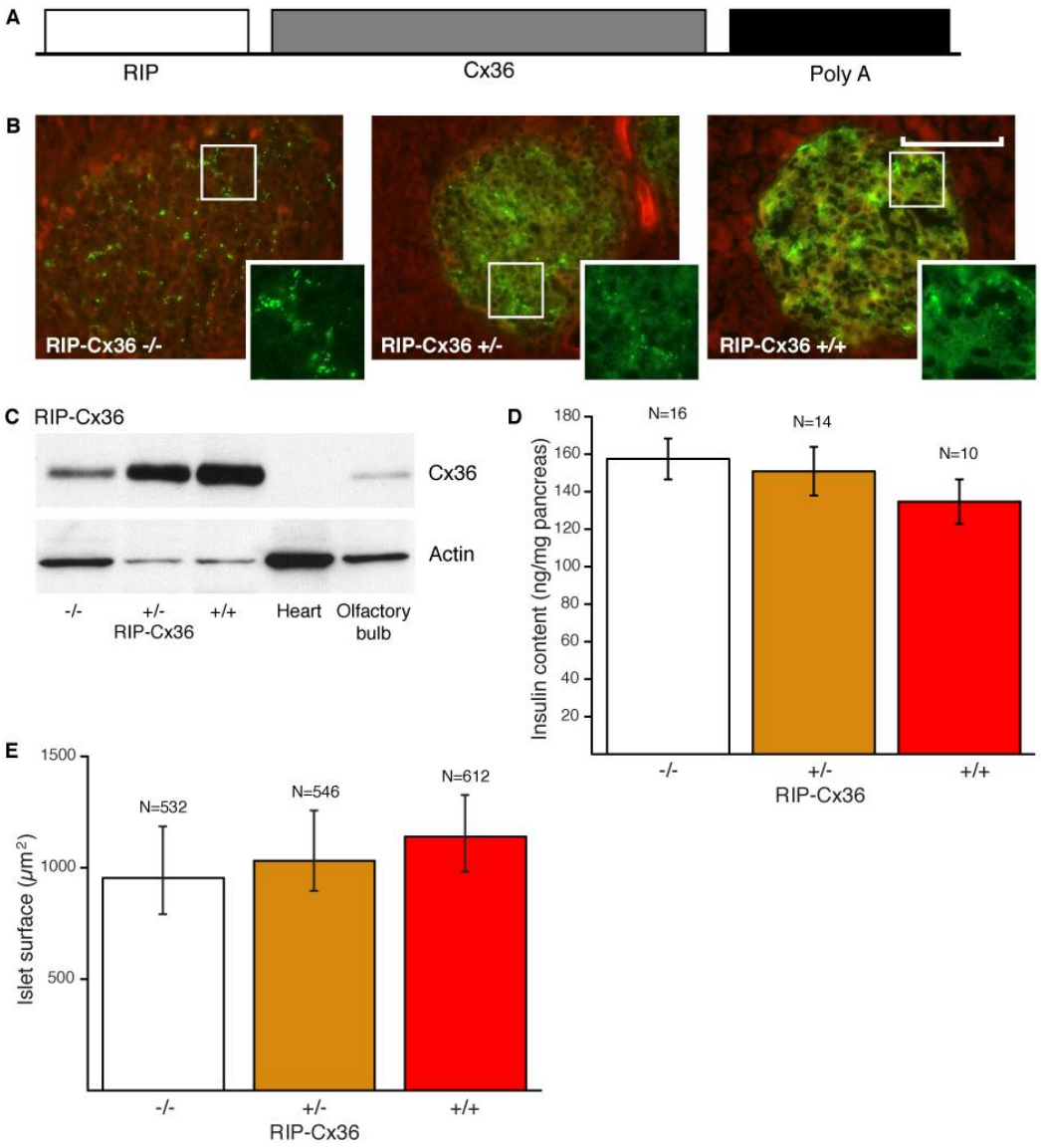

Figure S4: The β-cells of RIP-Cx36 mice feature higher levels of Cx36 and insulin than controls

A) To generate RIP-Cx36 transgenic mice we used (14) a 460-bp RIP sequence, a cDNA coding mCx36 (without the intron of the *Gjd2* gene), and sequences from either human GH (hGH) or β-globin (Poly A). Initial experiments were performed with the RIP-Cx36-hGH line. Experiments testing cytokines were performed with both the RIP-Cx36-GH and -β globin lines. The results did not reveal significant differences between the 2 lines. **B)** Immunofluorescence revealed the punctate distribution of Cx36 within an islet of a RIP-Cx36-/- mouse (left panel). This pattern was preserved in the islets of RIP-Cx36+/- (middle panel) and +/+ mice (right panel), which further showed increased cytoplasmic staining for Cx36. The boxed area is shown at higher magnification in the insets, under selective FITC illumination. Bar, 60 µm, 35 µm for insets. **C)** Immunoblot of total proteins revealed increasing levels of the protein in the islets of RIP-Cx36+/- and +/+ littermates. Ten µg total proteins were loaded per lane. The bottom panel shows the corresponding α-actin immunostaining. **D)** Radioimmunoassay showed a comparable insulin content of all RIP-Cx36 mice. Values are mean + SE of the indicated number of mice. **E)** Morphometric evaluation did not reveal significant differences in islet size between the 3 RIP-Cx36 genotypes, Values are medians +/- median error of the indicated number of islets,

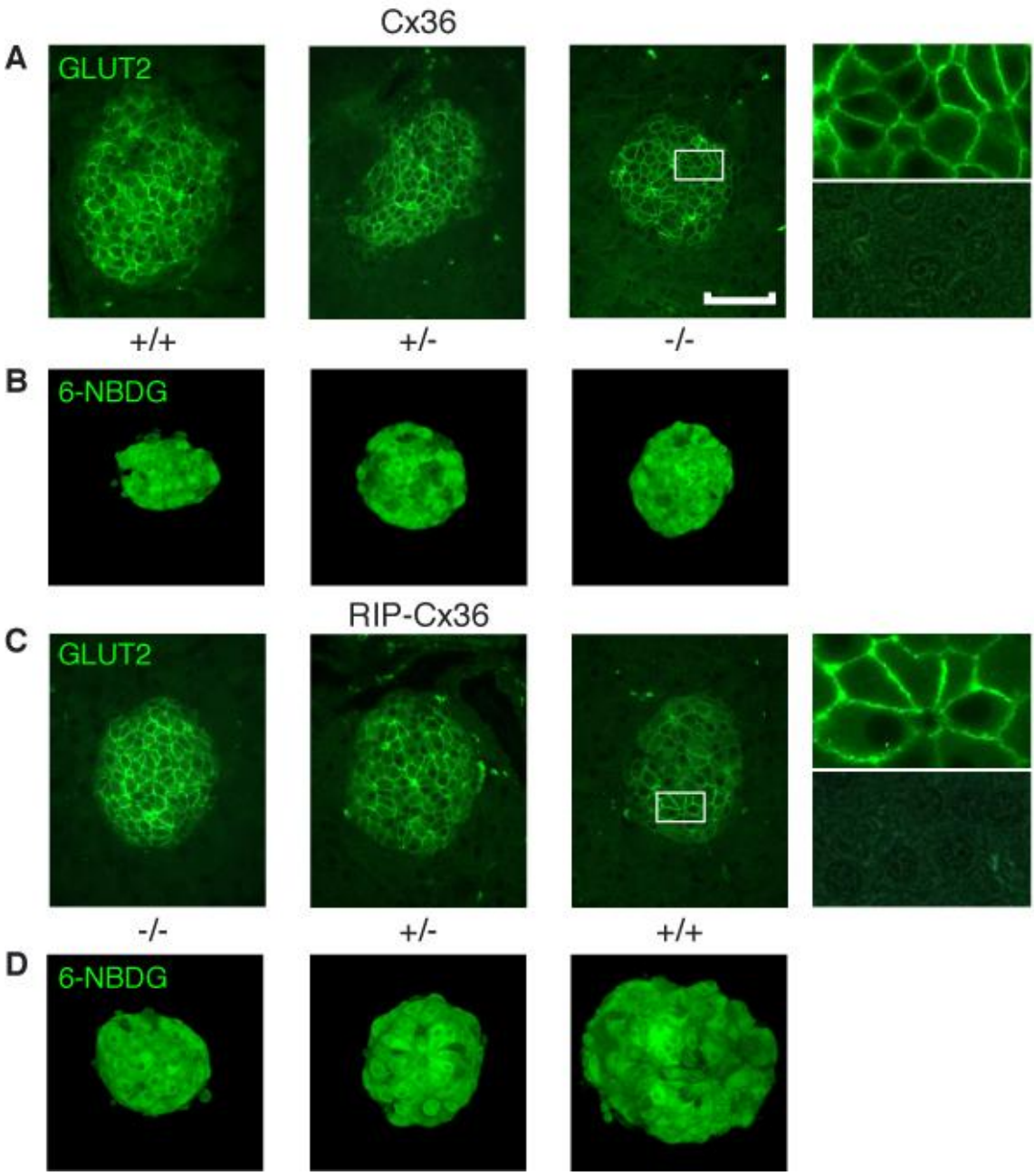

Figure S5: β-cells of Cx36 and RIP-Cx36 mice show similar GLUT-2 expression and glucose uptake

A) Immunolabeling revealed the presence of the GLUT2 glucose transporter, on the membrane of most β-cells in Cx36+/+, Cx36+/- and Cx36-/- islets. The boxed area is enlarged in the inset, and the bottom right enlargement shows the negative control. **B)** The actual uptake of glucose was tested in islets exposed to 0.7 mM 6-NBDG. After a 30 min incubation at 37ºC, this fluorescent glucose analogue was also incorporated by most β-cells of the islets of all Cx36 mice. **C and D)** Similar observations were made in the mice of the RIP-Cx36 line. Bar, 110 µm in A and C, 180 µm in B and D, and 25 µm in insets.

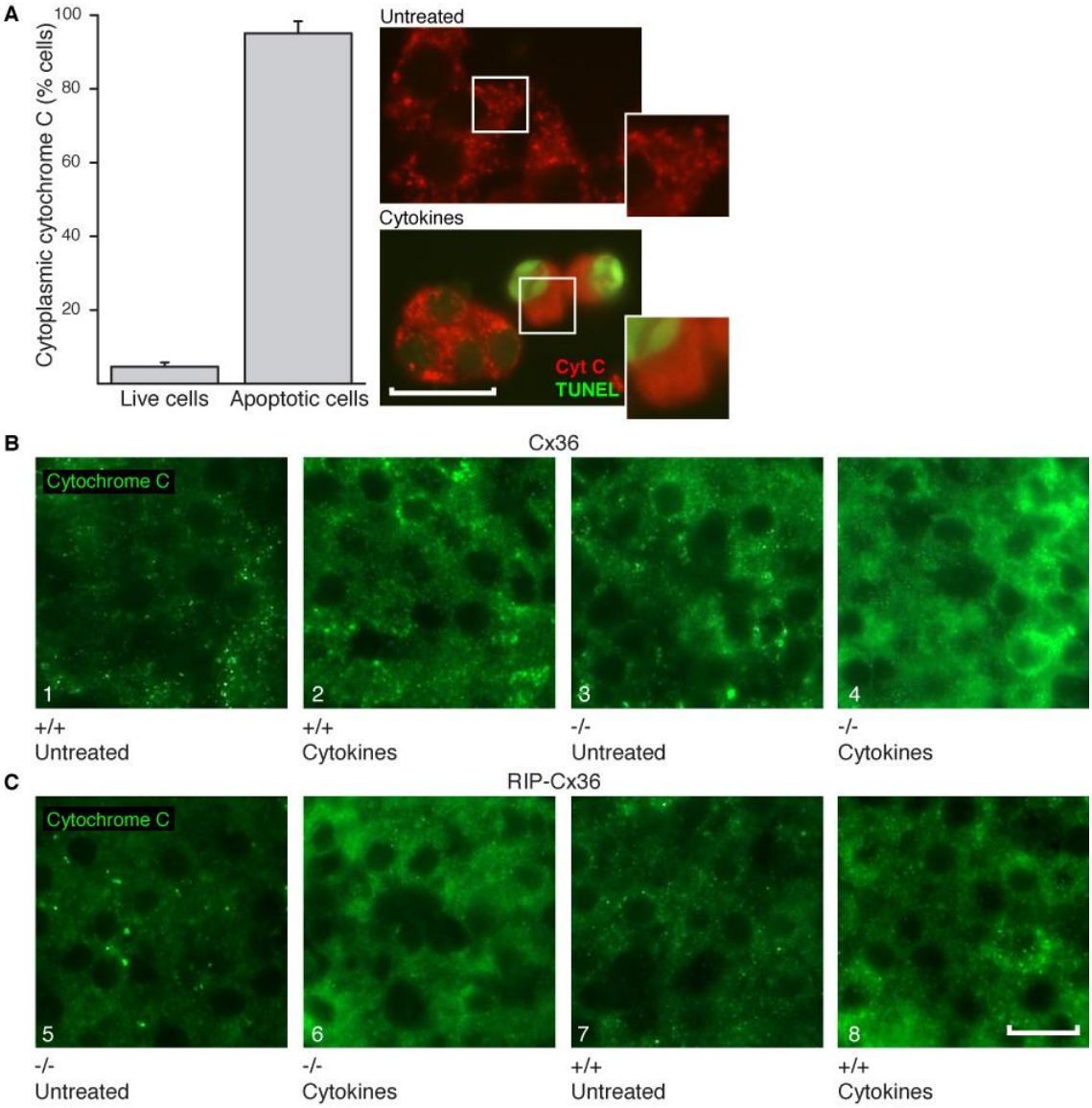

Figure S6: Pro-apoptotic cytokines cause a mitochondrial leakage of cytochrome C in MIN6 cells and isolated islets.

A) Cytochrome C (red) was detected at minute spots in control MIN6 cells, consistent with the mitochondrial distribution of the enzyme (top right panel). After exposure to the Th1 cytokines, many MIN6 cells featured a more homogeneous cytoplasmic labeling, consistent with the release of cytochrome C into the cytosol (bottom right panel). The left panel shows the mean + SE percentage of these cells in 3 experiments). Almost all these cells also featured a TUNEL positive signal (green nucleus), indicating that they were apoptotic (bottom right panel). The insets show enlargements of the boxed areas. B) After a 24h culture, islets isolated from Cx36+/+ mice showed a punctate immunostaining for cytochrome C (panel 1). This staining was not markedly affected after exposure to a mix of Th1 cytokines (panel 2). A similar pattern was observed in untreated islets of Cx36-/- mice (panel 3). In contrast, when these islets were exposed to cytokines, a more homogeneous, cytoplasmic staining was observed (panel 4). **C)** Analogous cytokine-induced changes were observed in control RIP-Cx36-/- mice (panels 5 and 6). In contrast, islets of RIP-Cx36+/+ mice exposed to cytokines (panel 8) retained the punctuate staining of cytochrome C observed under control conditions (panel 7). Bar, 25 µm

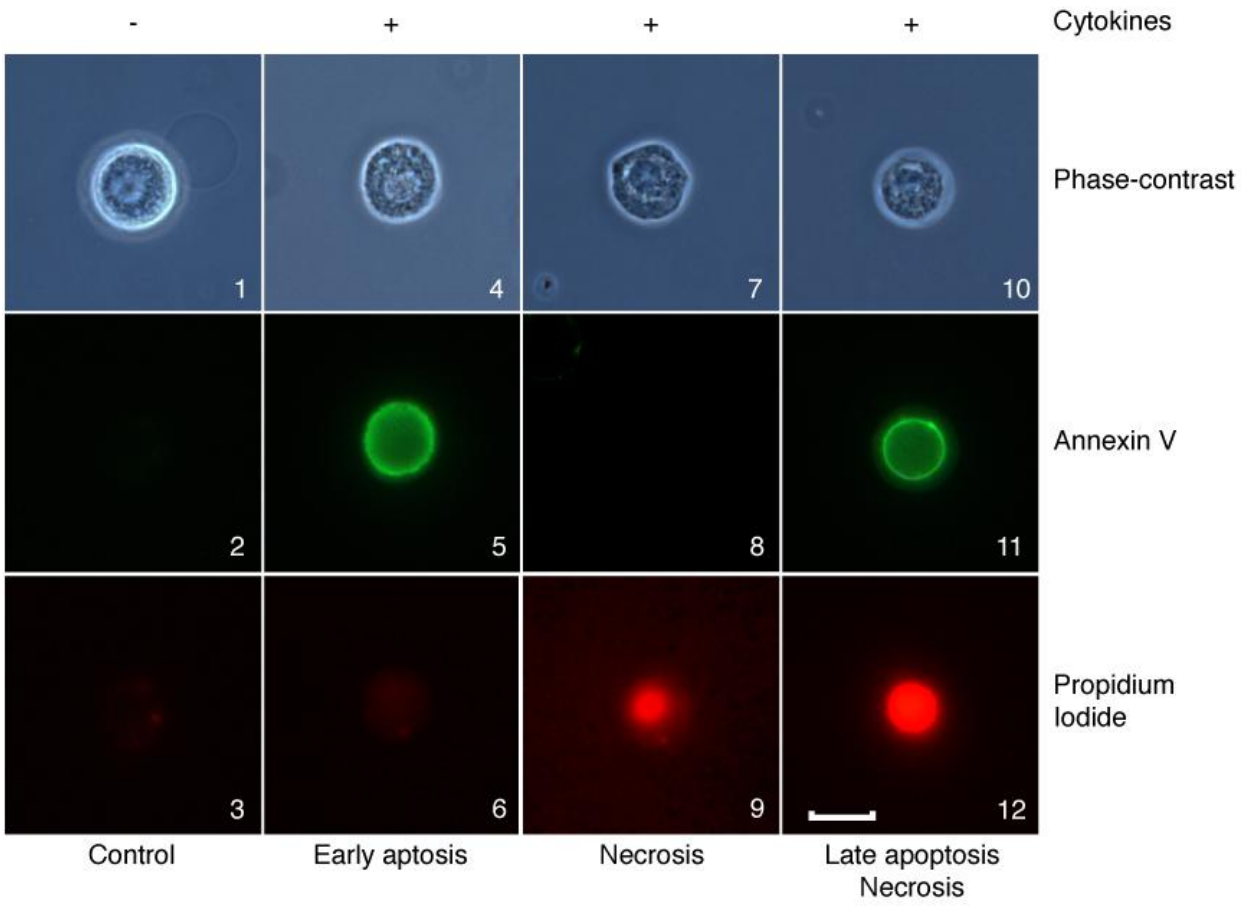

Figure S7: Cytokines kill single mouse β-cells by apoptosis and necrosis
Phase-and fluorescence views of single primary β-cells cultured for 36 h in the absence (-) or presence (+) of IL1-β, TNF-α and IFN-γ. Living β-cells featured a highly refringent outline (panel 1), and were negative under both FITC- (Annexin V-EGFP labelling; panel 2) and RH-fluorescence illumination (Propidium iodide labelling; panel 3). Dead β-cells had a fainter to nil refringent outline (panels 4, 7 and 10), and featured either an Annexin V-EFGP stained-membrane (panel 5), a propidium-iodide stained nucleus (panel 9), or a combination of the 2 labelings (panels 11 and 12), depending on whether they had been photographed in the early stages of apoptosis (panels 4-6) and necrosis (panels 7-9), or long after these processes had been initiated (panels 10-12). Bar, 12 μm.

Figure S9. Number of injections showing coupling

Mouse genotype	Lucifer Yellow No coupling	Lucifer Yellow Coupling (%)	Ethidium Bromide No coupling	Ethidium Bromide Coupling (%)	Chi Square Value Significance
Cx36 +/+	3	9 (69.2)	2	10 (83.3)	0.71 NS; 18.10 p < 0.001; 20.20 p < 0.001; 2.20 NS; 1.09 NS; 3.94 NS; 2.09 NS; 1.86 NS; 0.53 NS; 3.51 NS; 0.68 NS
Cx36 +/-	6	9 (60.0)	3	13 (81.2)	
Cx36 -/-	6	0 (0)	6	0 (0)	
RIP-Cx36 -/-	3	9 (75.0)	2	15 (88.2)	
RIP-Cx36 +/-	2	7 (77.8)	2	20 (90.9)	
RIP-Cx36 +/+	2	17 (89.5)	1	18 (94.7)	
RIP-Cx43 -/-	4	8 (66.7)	2	7 (77.7)	
RIP-Cx43 +/+	1	12 (92.3)	1	11 (91.6)	
RIP-Cx32 -/-	2	10 (83.3)	1	6 (85.7)	
RIP-Cx32 +/+	1	7 (87.5)	1	7 (87.5)	

The number of injections showing retention of each tracer in the injected cell (no coupling) and its diffusion in adjacent cells (coupling) were compared between the different mouse groups using the Chi square test. NS = not significant.

Figure S8: The proportion of microinjections revealing β-cell coupling was similar in all mice, but Cx36-/-.

The table shows the number of microinjections resulting in retention of either Lucifer Yellow or Ethidium Bromide within the injected cell (no coupling), and of those that resulted in the cell-to-cell transfer of either one of these 2 tracers into neighboring β-cells (coupling). The differences between groups in the occurrence of these 2 situations were evaluated by the Chi square test. Cx36-/- mice, which lacked Cx36, were significantly different from their +/- and +/+ littermates, which expressed Cx36. In all other lines, no significant difference in the number of coupling cases was observed between the genotypes that were compared.

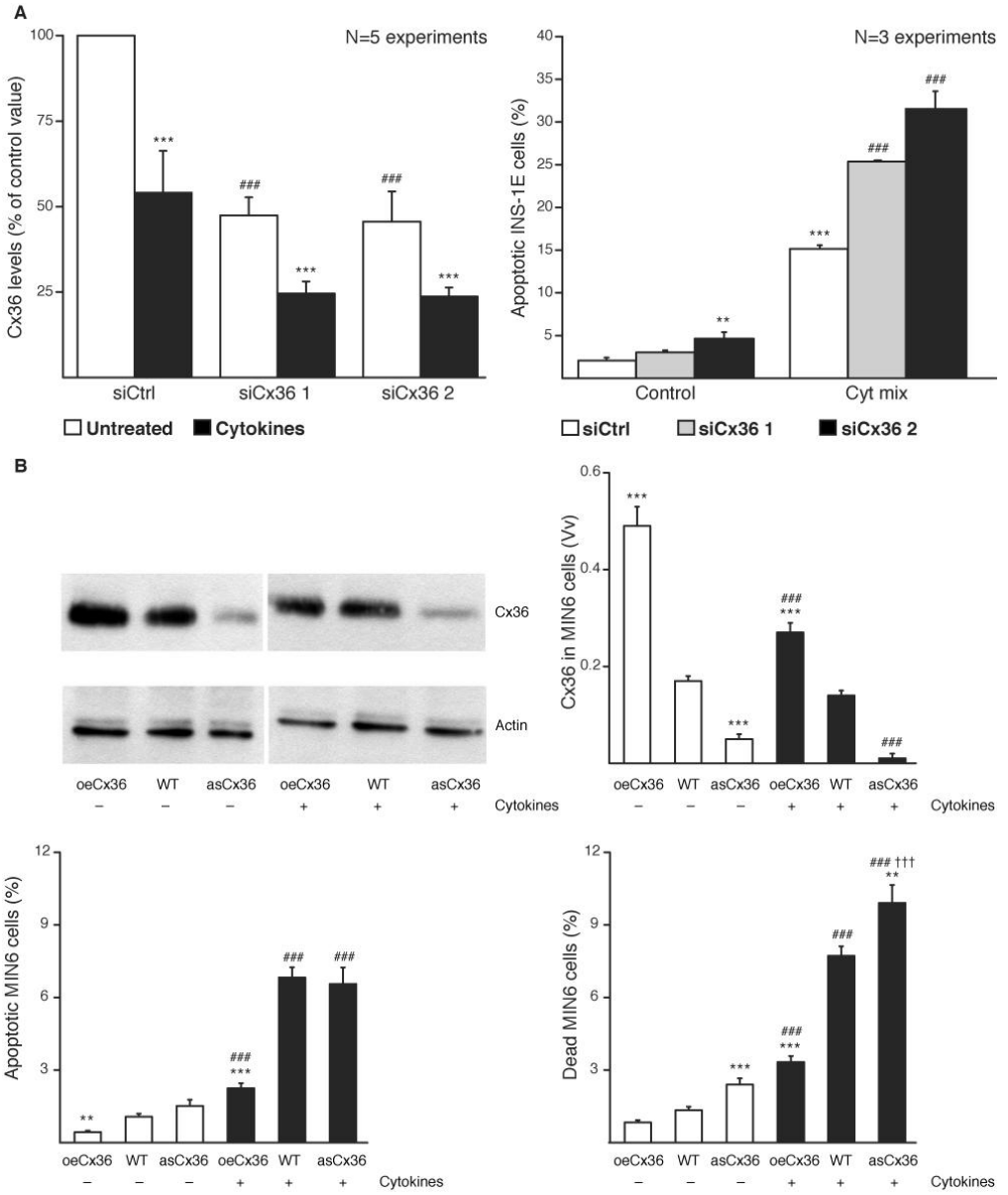

Figure S9: Th1 cytokines decrease Cx36, and alterations in Cx36 modulate apoptosis.
A) Left: 2 siRNAs targeting Cx36 (siCx36 1 and 2) decreased the expression of Cx36 protein in INS1-E cells (open columns; siCtrl = irrelevant siRNA). In all cells, exposure to cytokines further decreased Cx36 (solid columns). Values are mean + SE of 5 experiments. $^{###}$p<0.001 vs untreated siCtrl. *** p<0.001 vs corresponding untreated group. Right: after exposure to Th1 cytokines, siCx36-transfected cultures featured a higher percentage of apoptotic cells than control cultures. Data are mean + SE of 3-6 experiments. **p<0.008, ***p<0.001 vs. untreated control. $^{###}$p<0.001 vs. respective cytokine-treated siCtrl. **B)** Left top: Cx36 over expressing MIN6 cells (oeCx36) featured higher levels of Cx36 than wild type cells (WT), which had more Cx36 than cells transfected with an antisense Cx36 cDNA (asCx36). Lanes were run on a same gel but were not contiguous. Right top: These differences were confirmed by quantification of Cx36 immunofluorescence labeling. Data are mean + SE of 4 experiments. ***p<0.001 vs. untreated WT. $^{###}$p<0.001 vs. cytokine-treated WT. Left bottom: the proportion of apoptotic cells increased in all cells after exposure to cytokines. Under control and treated conditions, this proportion was lower in oeCx36 than WT and asCx36 cells. Data are mean + SE of 3-6 experiments. **p<0.005, ***p<0.005 vs. untreated WT, $^{###}$p<0.001 vs. corresponding untreated cell type. Right bottom: the proportion of dead cells (apoptosis plus necrosis) increased in all cells after exposure to cytokines. Under control and treated conditions, this proportion was higher in asCx36 than WT and oeCx36 cells. Data are mean + SE of 3-6 experiments. ***p<0.001 vs. untreated WT. $^{###}$p<0.001 vs. corresponding untreated cell type, †††p<0.001 vs cytokine-exposed oeCx36 and WT cells.